

Erdheim-Chester disease of multisystem involvement with delayed diagnosis: A case report and literature review

XIAOTONG SHI^{1*}, GUANGZHI SUN^{2*}, TONGGUAN LI³, MENGJIAO XU³,
YIXUAN LIU¹, ZHANKUI WANG⁴ and YANFENG HOU⁴

¹School of Clinical Medicine, Shandong Second Medical University, Weifang, Shandong 261053; ²Department of Orthopedic Surgery, The First Affiliated Hospital of Shandong First Medical University and Shandong Provincial Qianfoshan Hospital, Shandong Key Laboratory of Rheumatic Disease and Translational Medicine, Jinan, Shandong 250000; ³The First Affiliated Hospital of Shandong First Medical University and Shandong Provincial Qianfoshan Hospital, School of Clinical Medicine, Shandong First Medical University, Jinan, Shandong 250117; ⁴Department of Rheumatology and Autoimmunology, The First Affiliated Hospital of Shandong First Medical University and Shandong Provincial Qianfoshan Hospital, Shandong Key Laboratory of Rheumatic Disease and Translational Medicine, Shandong Medicine and Health Key Laboratory of Rheumatism, Jinan, Shandong 250000, P.R. China

Received May 31, 2023; Accepted January 30, 2024

DOI: 10.3892/etm.2024.12447

Abstract. Erdheim-Chester disease (ECD) is a rare tumor of histiocytic origin, characterized by foamy or lipid-laden histiocytes mixed or surrounded by fibrosis that infiltrate multiple organs. Misdiagnosis is common due to the diversity of clinical presentations. The present study reported a case of ECD with the involvements of bone, cardiac, aorta and retroperitoneum. The patient had no obvious clinical symptoms and no noteworthy foamy histiocytes or Touton giant cells were found on pathological examination, delaying the diagnosis. The patient was a young male found to have pericardial effusion on physical examination, and computed tomography (CT) revealed soft tissue infiltrates in the retroperitoneum and around the aorta. A mediastinal biopsy revealed fibrous connective tissue with small-vessel hyperplasia and acute-chronic inflammatory cell infiltration. The initial diagnosis was retroperitoneal fibrosis (RPF), and hormonal and tamoxifen treatments were administered. The patient presented with oliguria, eyelid edema and fever four

years later. A repeat CT revealed an increase in the extent of tissue infiltration and pericardial effusion compared with the previous CT. Subsequent cardiac magnetic resonance imaging revealed massive thickening in the form of fibrotic tissue infiltrating the heart and surrounding thoracic and abdominal aorta. Single photon emission CT revealed multiple areas of increased bone metabolism, particularly symmetrical involvement of the long bones of both lower extremities. A biopsy of the perirenal tissue revealed fibrous tissue and a small number of lymphocytes and macrophages [typical foamy histiocytes observed via x200 magnification and hematoxylin-eosin (HE) staining, no presence of xanthogranuloma or Touton giant cells]. After a comprehensive evaluation and ruling out other diseases, the diagnosis of ECD was determined. The prognosis of this disease is poor; early diagnosis is critical and requires accurate judgment by clinicians. Biopsies of all involved sites and refinement of genetic tests to guide treatment, if possible, are both necessary.

Introduction

Erdheim-Chester disease (ECD), also known as non-Langerhans histiocytosis, is a rare histiocytic neoplasm in which >50% of patients have BRAF mutations (1-3). The disease is prevalent in middle-aged and older adults, with a median age of onset of 55 years (4). The 5-year survival rate of the disease is 68%, and most deaths result from involvement of vital organs, including the heart and central nervous system (5). Symmetrical osteosclerosis of the long bones of both lower extremities occurs in >95% of patients, only half of whom may experience bone pain. In addition, ECD may be accompanied by other systemic manifestations, such as oliguria and dysuria in perirenal infiltration, periaortic inflammation in aortic involvement, myocarditis, arrhythmia, heart failure and even myocardial infarction in cardiac involvement, ataxia and diabetes insipidus in neurological involvement and macular

Correspondence to: Dr Yanfeng Hou or Dr Zhankui Wang, Department of Rheumatology and Autoimmunology, The First Affiliated Hospital of Shandong First Medical University and Shandong Provincial Qianfoshan Hospital, Shandong Key Laboratory of Rheumatic Disease and Translational Medicine, Shandong Medicine and Health Key Laboratory of Rheumatism, 16766 Jingshi Road, Jinan, Shandong 250000, P.R. China
E-mail: yfhou1016@163.com
E-mail: 2122@sdsdhospital.com.cn

*Contributed equally

Key words: Erdheim-Chester disease, atypical pathology, pericardial effusion, hairy kidney, case report

tumors in skin involvement (3). Misdiagnosis is common as the condition affects multiple systems and manifests variably in different patients (6).

Typical pathologic features are that the lesion tissue is rich in foamy histiocytes surrounded by fibrosis or xantho-granuloma and Touton giant cells are often seen (2). Whereas immunohistochemistry (IHC) results show positive for CD68 and CD163 and negative for CD1a and Langerin (CD207) (2,3). Notably, a review of the literature revealed that pathological examination of some patients with ECD may only show fibrosis with nonspecific inflammatory cell infiltration while lacking typically foamy cells (3,7,8). Therefore, the diagnosis needs to be based on histopathology, combined with a comprehensive evaluation of clinical features, imaging and the exclusion of other diseases (2).

Pegylated interferon α (PEG-IFN- α) agents remain the first-line treatment for the disease; however, drugs which target mutation sites such as BRAF, MEK and mTOR inhibitors can improve survival in patients with positive genetic tests such as BRAF-V600E (3,9). These targeted agents often have toxicities associated with inhibition of the MAPK pathway (e.g., inducing a systemic inflammatory response) and thus have to be discontinued. However, combining PEG-IFN- α agents with interleukin 1 inhibitors (e.g., anakinra) can prolong the use of targeted agents by controlling toxicity and effectively mitigating the inflammatory response (10,11). Furthermore, corticosteroids can be used as adjuvants to improve acute symptoms associated with tissue swelling; however, they cannot improve survival rates (3,12). Owing to the multifocal nature and insensitivity of ECD to radiation, extensive surgery and radiotherapy are not recommended (13). Clinicians should increase awareness and diagnostic sensitivity of ECD, actively biopsy all patients with suspected ECD and all of their affected tissues, and perform genetic testing of diseased tissues to guide treatment (3). The options for therapy need to be individualized based on the sites of involvement, degree of disease progression, and genetic results (14). To aid in addressing the gaps in knowledge, the present study discussed a case report which details the diagnosis and treatment process of a patient with ECD.

Case report

Presentation. In early 2017, a 31-year-old man was admitted to the cardiology unit of Liaocheng People's Hospital (Shandong, China) and found to have a moderate asymptomatic pericardial effusion. Subsequently, a CT scan of the patient's chest, abdomen and pelvis was performed and the image showed aortic, mediastinal, and pericardial thickening and pleural effusions. Symptomatic treatments, including torasemide and spironolactone for diuresis, leading to a reduction of pericardial effusion; valsartan hydrochlorothiazide to lower blood pressure; metformin to lower glucose; and fluvastatin to lower lipids, were performed (the discharge records of that time did not contain detailed records of the exact dosages of the medications, or the number of days of their use; thus, it was not possible to present them in detail in the present study). However, the treatments provided no improvements regarding the pericardial effusion or retroperitoneal mass. Following this, the patient was transferred to the First Affiliated Hospital

of Shandong First Medical University (Shandong, China) for a mediastinal tissue biopsy which revealed fibrous connective tissue with small vessel hyperplasia and an infiltrate of acute-chronic inflammatory cells (images from this hospital were unavailable). The patient was diagnosed with suspected fibrous mediastinitis. The patient was not hospitalized for treatment and arrived at the Rheumatology Unit of the First Affiliated Hospital of Shandong First Medical University (Shandong, China) in April 2017 for further examination.

Subsequent CT (GE Discovery CT 750 HD; Cytiva) images revealed a retroperitoneal soft-tissue mass growing around the bilateral ureter, thoracic aorta, and part of the abdominal aorta (Fig. 1A and B). Blood test results showed the presence of an inflammatory response, as evidenced by a white blood cell (WBC) count of $14.54 \times 10^9/l$ (normal range: $3.5-9.5 \times 10^9/l$), neutrophil count of $9.99 \times 10^9/l$ (normal range: $1.8-6.3 \times 10^9/l$), erythrocyte sedimentation rate of 16 mm/h (normal range: 1-15 mm/h) and C-reactive protein (CRP) of 9.45 mg/l (normal range: 0-3.48 mg/l). Antinuclear and anti-neutrophilic cytoplasmic antibodies were negative. IgG4 levels and liver and kidney functions were within normal limits. Physical examination revealed no palpable masses or lymphadenopathy in the chest or abdomen. Based on these findings, RPF was diagnosed. The comorbidities of the patient included hypertension, type-2 diabetes and fatty liver, with no history of cancer or autoimmune disease and no family history of cancer or autoimmune disease. In order to reduce inflammation and shrink fibrotic masses, the patient was administered intravenous methylprednisolone 60 mg once daily for 11 days. Following this, the patient was administered oral prednisone 50 mg once daily and oral tamoxifen 10 mg three times daily for 7 days, which was subsequently changed to 20 mg three times daily. Thereafter, the patient presented to the First Affiliated Hospital of Shandong First Medical University twice for follow-up examinations. CT (GE Discovery CT 750 HD; Cytiva) showed that the retroperitoneal mass was unchanged. After 6 months, the patient felt that there was no improvement in his condition and discontinued oral corticosteroid therapy without consulting the physician.

The patient remained asymptomatic until November 2021, when the patient developed decreased urine output, bilateral eyelid edema and fever. A physical examination revealed distant heart sounds. Blood tests were unremarkable other than a WBC count of $13.21 \times 10^9/l$, neutrophil count of $10.0 \times 10^9/l$, CRP level of 19.4 mg/l and aspartate aminotransferase level of 18.6 U/l (normal range: 9-50 U/l). CT (GE Discovery CT 750 HD; Cytiva) images revealed expansion of the periaortic soft tissue mass (Fig. 1C and D). Echocardiography (Philips EPIQ 7C; Philips Medical Systems B.V.) revealed a large pericardial effusion with a heart swing syndrome (Fig. 2). No findings indicated any evidence of malignancy or tuberculosis. Subsequently, the patient received treatment for RPF, comprising intravenous methylprednisolone 40 mg (once daily) and oral tamoxifen 10 mg (twice daily). Pericardiocentesis was performed, allowing the drainage of 1,500 ml of pericardial fluid. The image obtained from a repeat cardiac ultrasound scan suggested trace pericardial effusion, thickening of the right ventricular lateral epicardium layer (to ~7 mm), and reduced right ventricular systolic function. After applying the above regimen for 6 days, the patient was discharged with improvement, and the hormone

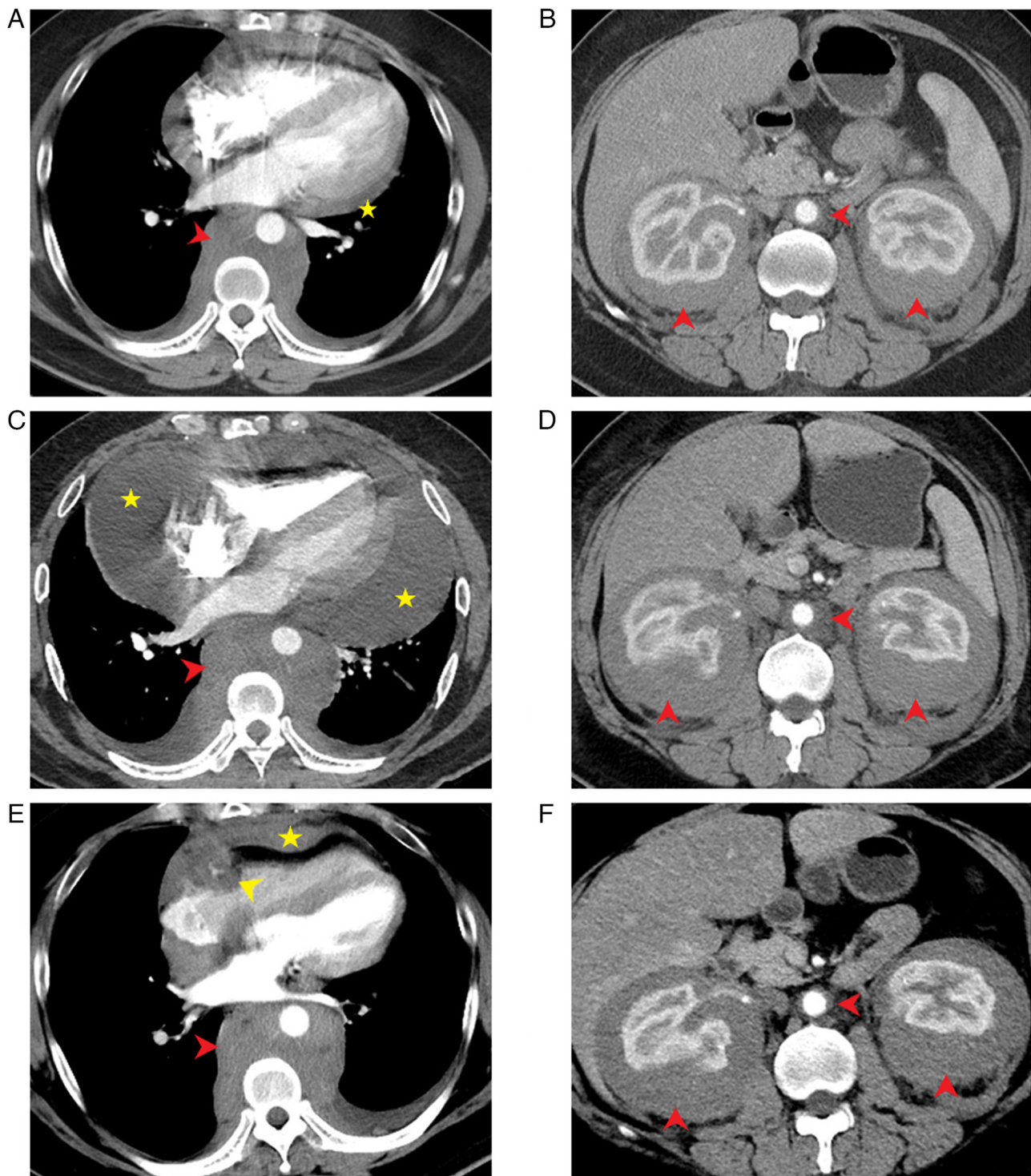


Figure 1. T2-weighted computed tomography images (axial view) of the chest and abdomen. (A and B) Images from 2017 showing the muscle-isodense tissue (red arrow) encircling the thoracic-abdominal aorta, the heart, and both kidneys, and a mild pericardial effusion (yellow star). (C and D) Images from 2021 showing a significant increase of tissue lesions (red arrow) and pericardial effusion (yellow star) compared with images from panels A and B. (E and F) Images from February 2023 showing lesions (red arrow) around the thoracic and abdominal aorta and pericardial effusion are reduced compared with images from panels C and D. A thickening of the lateral wall of the right heart (yellow star), pseudotumor, in the right atrioventricular groove, encircling the right coronary artery (yellow arrow), and significant compression of the heart.

therapies were switched to oral prednisone 50 mg (once daily), with a reduction of 1 tablet per week, and oral tamoxifen was adjusted to 20 mg (twice daily), with the addition of oral cyclophosphamide (once every other day) as a second-line agent for long-term maintenance therapy, and the patient was advised to repeat the examination after 1 month.

After 6 months of irregular oral treatment with the above medications, a repeat CT scan (Fig. 1B and E) showed no significant changes in the retroperitoneal mass in the patient. However, it was observed that the patient's aortic involvement was circumferential, which was inconsistent with an RPF diagnosis, as RPF only involves the anterior and lateral parts

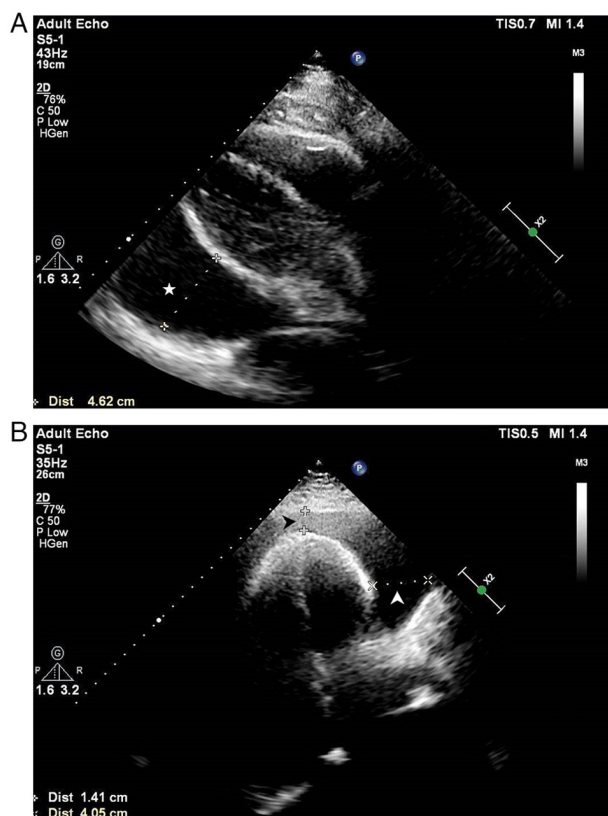


Figure 2. Echocardiography in November 2021. A large fluid-dark area was observed in the pericardial cavity. (A) The depth of effusion was 46 mm posterior to the left ventricle (white star), (B) 41 mm lateral to the left ventricle (white arrow) and 14 mm apical to the heart (black arrow).

of the aorta. Thus, it was considered that RPF might not be the most appropriate diagnosis for the present patient. The case was reviewed to develop new diagnostic and treatment options. During a review of the CT images, diffusely proliferating soft tissues involving the heart, thoracic and abdominal aorta and both kidneys were observed (Fig. 1A-F; red arrows). Specifically, the right atrioventricular groove pseudotumor, ‘coated aorta’ and ‘hairy kidney’ signs were observed, which are the typical imaging manifestations of ECD. Therefore, cardiac magnetic resonance (CMR; Philips Ingenia CX 3.0T; Philips Medical Systems B.V.) imaging, whole-body bone scanning (GE Infinia; Cytiva) and a biopsy of the perirenal tissue were performed. CMR imaging revealed a diffuse long T1 and slightly prolonged T2 signal around the mediastinum and pericardium. Lesion tissues encircled the large mediastinal vessels and the heart, resulting in significant cardiac compression. The right coronary artery was involved and the left ventricular diastolic function was visibly restricted. The findings were consistent with constrictive pericarditis (Fig. 3). Whole-body anteroposterior planar imaging performed via technetium methylene diphosphonate single-photon emission CT (99mTc-MDP-SPECT/CT) revealed increased bone metabolism in the right lower femur and bilateral tibia and slightly increased bone metabolism in the left sixth anterior rib, thoracolumbar body, bilateral sacroiliac joint and bilateral hip joint (Fig. 4). While puncturing the perirenal tissue, it was found that the tissues were very dense. Due to the difficult penetration of the puncture needle to penetrate deep into the

tissue, a small quantity of tissue samples were obtained from the lesion surface. The pathological result showed hyperplastic dense fibrous connective tissue with scattered individual lymphocytes and phagocytes (HE staining, magnification, x100; Fig. 5A). To avoid the risks associated with multiple invasive surgeries, biopsies were not performed on all diseased tissues. Since no histiocytes were found, IHC or genetic testing were not performed on the pathologic tissues. Thus, differential diagnosis was critical.

Differential diagnosis. The patient's physical examination and ancillary findings did not support conditions, such as malignancy, tuberculosis, heart failure and liver disease, and other diseases that may result in pericardial or pleural effusions, or diseases, such as lymphoma, sarcoma, IgG4-related disease, and multiple myeloma, which may result in retroperitoneal masses. The ‘coated-aorta’ on CT can exclude diseases involving the aortic wall, such as Takayasu disease, Horton disease, and infectious aortitis. In differentiating RPF from ECD, the presentation of bilateral lower extremity bone hypermetabolism, ‘hairy kidney’, and circumferential changes of aorta on CT were more supportive of an ECD diagnosis. At this point, the diagnosis was still uncertain. Thus, the pathological images were reviewed again and some typical foamy histiocytes of ECD surrounded by fibrosis were found when the magnification was adjusted to x200 and x400 (Fig. 5B and C). Hematological and cranial examinations did not reveal any involvement of the adrenal glands, pituitary gland, central nervous system, or orbit. Finally, the patient was diagnosed with ECD. IFN- α therapy was recommended; however, the patient declined this option and chose to continue hormone and cyclophosphamide treatment with regular follow-up CT scans.

Outcome and follow-up. A recent CT (GE Revolution CT; Cytiva) performed in February 2023 revealed smaller lesions around the thoracoabdominal aorta compared with the previous findings (Fig. 1E and F). After re-communication, the patient consented to the administration of subcutaneous PEG-IFN- α -2b 135u (once weekly), oral prednisone 20 mg (once daily), oral tamoxifen 10 mg (twice daily) and oral cyclophosphamide 50 mg (once every other day) from February 2023. Until January 2024, the patient has consistently adhered to this regimen of treatment without experiencing any discomfort. The patient has been advised to come to the hospital for review at the patient's convenience.

Radiographic technique. The present study selected images of the phase-sensitive inversion recovery turbo field echo breath-hold (PSIR-TFE-BH) sequence and the sense-balanced turbo field echo-BH-cine sequence obtained using Philips Ingenia CX 3.0T scanners (Philips Medical Systems B.V.). The PSIR-TFE-BH parameters were as follows: Repetition time, 6.13 msec; echo time, 2.99 msec; slice thickness, 2 mm; scan percentage: 74.1%; TFE factor, 20; TFE shots, 6; field of view (FOV), 300 mm, 233.3 Hz; ACQ matrix MxP, 188x139; and scan time, 13 sec. The sBTFE-BH-cine parameters were as follows: repetition time, 2.7 msec; echo time, 1.36 msec; slice thickness, 3 mm; scan percentage: 94.7%; TFE factor, 18; TFE shots, 5; FOV,

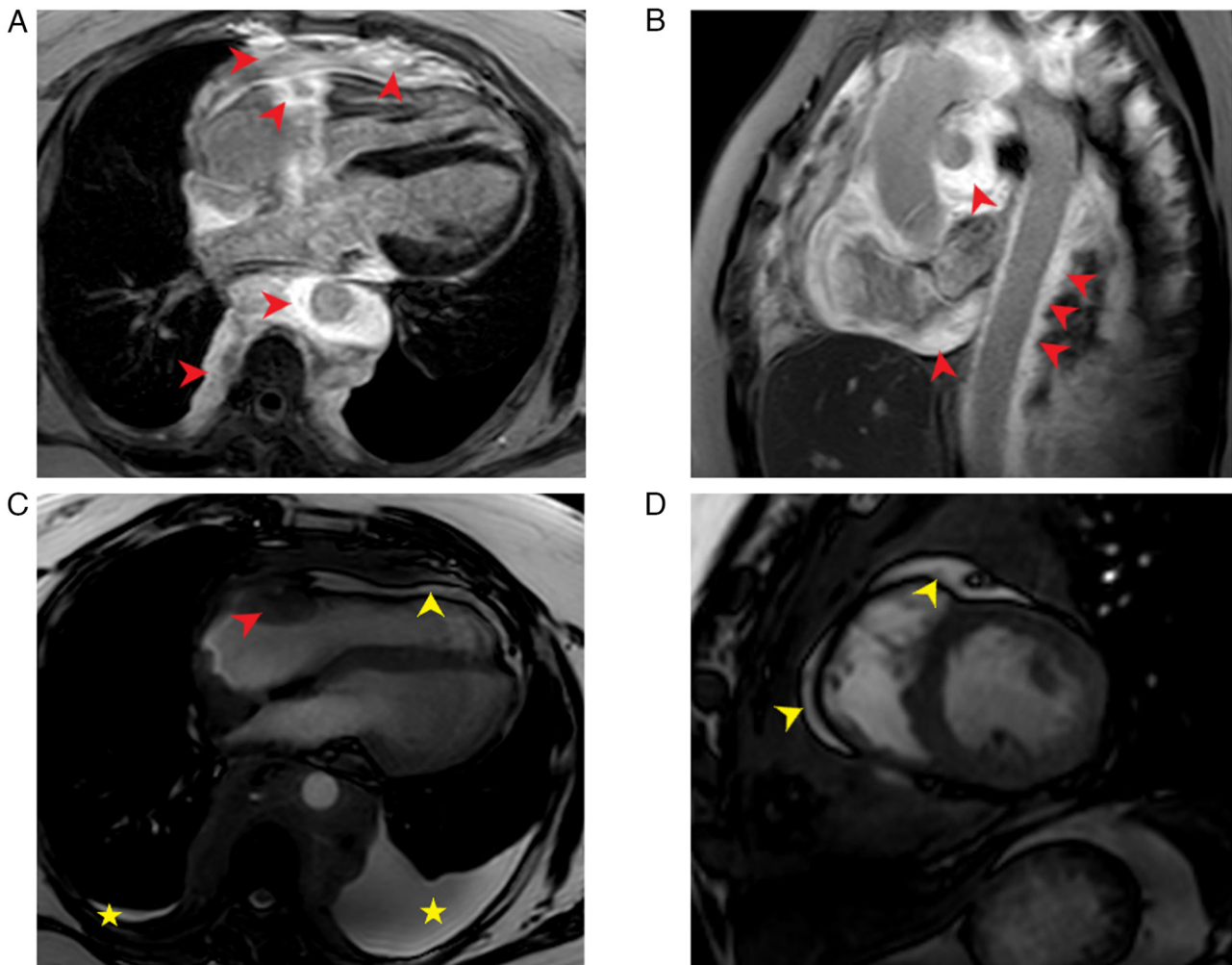


Figure 3. Cardiac magnetic resonance images. (A) PSIR-TFE four chamber view showing abnormal high signal around the aorta and right coronary artery, and abnormal mixed high signal in the posterior mediastinum and lateral right heart, suggestive of tissue infiltration of Erdheim-Chester disease (red arrow). (B) PSIR-TFE sagittal view shows massive thickening (non-homogeneously enhanced density) encircling the entire heart and spreading from the aortic root to the abdominal aorta (red arrow). (C) Steady state free precession four chamber view and (D) short axis view showing a mild pericardial effusion (yellow arrow) and pleural effusion (yellow star). PSIR-TFE, phase-sensitive inversion recovery turbo field echo.

300 mm, 1442.6 Hz; ACQ matrix MxP, 152x144; and scan time, 6 sec. The GE Infinia camera system (Cytiva) was used for SPECT. The reagent used was 99mTc-MDP; route, intravenous injection; dose, 20 mCi; time elapsed, 4 h; scan area, anterior and posterior position; collimator, low-energy high-resolution; collimator mode, H mode; enter machine mode, enter head-first; energy peak, 140 keV; time, 10 min. The GE Discovery CT 750 HD scanner (Cytiva) was used for CT; scan type, helical; voltage, 120 kV; routine time, 0.7 sec; scan duration, 9.62 sec; detector coverage, 40 mm; helical thickness, 5 mm; coverage speed, 56.25 mm/sec; pitch, 0.984:1. The GE Revolution CT scanner (Cytiva) was also be used; scan type, helical; voltage, 120 kV; routine time, 0.5 sec; scan duration, 12.30 sec; detector coverage, 80 mm; helical thickness, 5 mm; coverage speed, 158.75 mm/sec; pitch, 0.992:1. The Philips EPIQ 7C system (Philips Medical Systems B.V.) was used with the following specifications employed for echocardiography: model, Adult Echo; ultrasound probe, S5-1; ultrasonic frequency, 43 Hz; penetration distance, 19 cm; thermal index of soft tissue, 0.7; mechanical index, 1.4.

Literature search. A search of PubMed (<https://pubmed.ncbi.nlm.nih.gov>) was performed using the keywords 'Erdheim-Chester' or 'non-Langerhans,' 'retroperitoneal fibrosis' or 'idiopathic retroperitoneal fibrosis' or 'chronic peri-aortitis,' 'hairy kidney,' 'coated-aorta,' 'pericardial effusion,' 'histiocytosis,' 'Langerhans,' and 'Rosai Dorfman', for English publications up to October 20, 2023, without other restrictions on publication date. The reference sections of the included articles were also searched and the titles and abstracts from all sources screened.

Discussion

ECD is a rare form of non-Langerhans histiocytosis characterized by mutant clonal histiocytes that provoke nonspecific fibrosis and inflammation followed by infiltration of long bone marrow and/or tissues of a number of other organs (3). *BRAF* is a common mutation site, occurring in >50% of patients with ECD, with the primary affected pathway being MAPK-ERK. The identification of gene mutations provides evidence for their clonal properties (2). As systemic

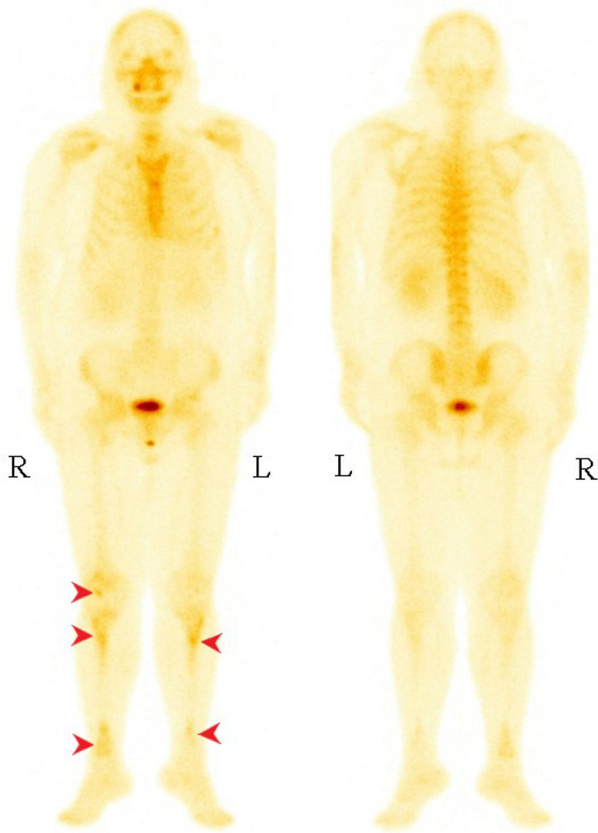


Figure 4. 99mTc-methylene diphosphonate-single photon emission/computed tomography images. 99mTc-methylene diphosphonate-single photon emission/computed tomography anteroposterior view demonstrating increased bone metabolism at the right lower femur and bilateral tibias (red arrow).

histiocytosis, ECD, along with Langerhans cell histiocytosis (LCH) and Rosai-Dorfman disease (RDD), have been classified as low-grade histiocytic/dendritic neoplasms in the fifth edition of the World Health Organization Classification of Hematolymphoid Tumors (1). By 2024, >1,500 cases of ECD are estimated to have been reported in the medical literature. Early diagnosis is challenging due to its broad and nonspecific clinical presentation, low prevalence, inconsistent pathological findings, and lack of clinician awareness of the disease (7,15).

The typical pathology of ECD is characterized by a diffuse infiltrate of foamy or lipid-laden histiocytes admixed or surrounded by fibrosis or xanthogranuloma and Touton giant cells are often present (3,8). The histiocytes are positive for CD68 and CD163 (the macrophage or dendritic cell markers, which are also positive in LCH and RDD), negative for CD1a and Langerin (CD207; which are typically positive in LCH), and negative or weakly positive for the S-100 protein (which is positive in RDD) (2). This tissue pathology can affect a number of organs due to its susceptibility to connective, adipose, and perivascular tissues (6). At the molecular level, in addition to the most common *BRAF600E* mutation, other MAPK pathway-related genes, such as *PIK3CA*, *MAP2K1*, *N/KRAS* and *MAP3K1*, are also involved (14). The presence of *BRAF* mutations, which has a similar probability in ECD and LCH, but rarely in other histiocytosis, can be useful for differentiating ECD from other non-LCH (8,15). In a study

by De Abreu *et al*, histological analysis revealed a much greater extent of ECD than that revealed by magnetic resonance imaging (MRI) or radiology (16). Variable components include histiocytic infiltrates and the surrounding stroma (3). It has also been suggested that the *BRAF* mutation rate could be 100% if every patient with ECD completed genetic testing (8). Therefore, biopsies of lesion tissues and genetic testing should be performed in all cases of ECD to confirm the diagnosis and establish the mutational status to potentially guide therapy (3). Moreover, the *BRAF* mutations are expressed in foamy tissue and Touton giant cells, but not in fibroblasts, lymphocytes, or endothelial cells, suggesting a need for multiple core biopsies and to expand the scope of lesion biopsies to optimize tissue yield for histopathological review and molecular testing (3,17).

In the present case, tissue biopsies were performed at different times on two different lesion sites that showed only fibrosis with inflammatory cell infiltration, lacking the typical histiocytes of ECD, which poses a diagnostic challenge. The literature was reviewed (3,7,8) and it was found that the ECD histopathology may lack the typical foamy histiocytes and show only nonspecific inflammation mixed with fibrosis or even only fibrosis lamellae mixed with a few histiocytes, which is consistent with both of the biopsies in the present study. Therefore, the ECD diagnosis cannot be made solely based on pathologic findings; instead, it necessitates clinicoradiological manifestations and the exclusion of other diseases (2).

ECD primarily occurs in middle-aged to older adults, with a male:female ratio of 3:1, and can affect almost all organ systems (4,5). Symmetric long bone involvement is the most common symptom and can occur in 95% of cases, showing cortical thickening, metaphyseal medullary sclerosis of the tubular bones and coarse trabeculations on radiographs (8). It might be overlooked because only 50% patients present with bone pain (3). Although rare, the involvement of the cranial and facial bones, clavicle, sternum, ribs, scapula, pelvis and spine has also been reported (18). The patient in the present study did not present with bone pain during the course of the disease; nevertheless, a typical symmetric metabolic increase in long bones was found after performing the 99mTc-MDP-SPECT/CT. This suggested that clinicians should supplement the assessments with a whole-body bone or PET-CT scan to evaluate long bone involvement as early as possible when patients are suspected of having ECD due to other clinical manifestations. In addition, an MRI of long bones may be informative in revealing epiphyseal involvement and periostitis, which are often overlooked on plain films (8).

Extraskelletal manifestations, such as perirenal infiltrates, cardiac pseudotumors, periaortic sheaths, protruding eyeballs, yellow tumors of the eyelids and involvement of the lungs, nervous system and skin are present in ~50% of the patients (19). The involvement of cardiac or neurologic systems in ECD usually has a poor prognosis (14).

Tissue infiltration of thoracic involvement in ECD can involve all anatomic areas from the pleura to the periaortic region and may appear as a thickening of the visceral pleura and pseudotumoral mass (20). The incidence of this infiltration occurring in the cardiovascular system is 40-70% (3,14). Vascular involvement typically shows tissue infiltration from the ascending aorta to the iliac artery junction, creating a 'coated aorta' on CT (19). Unlike Takayasu disease, Horton

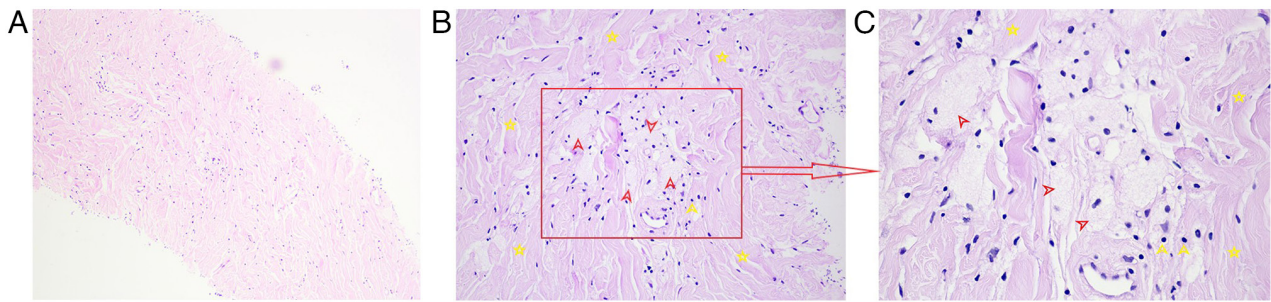


Figure 5. Histopathological appearance of perirenal infiltration. (A) Low magnification; dense fibrotic tissue, magnification, x100; H&E staining. (B) A partially enlarged view of panel (A); foamy histiocytes (red arrow) with surrounding fibrosis (yellow star) can be seen, magnification, x200; H&E staining. (C) A partially enlarged view of panel (B); foamy histiocytes look more evident, magnification, x400; H&E staining. H&E, hematoxylin and eosin.

disease, and infectious aortitis, which may involve the entire aortic wall, ECD tissue infiltration involves only the space around the outer aortic membrane. This infiltration is circumferential rather than anterior or lateral to the aorta, sparing the posterior aspect, as in RPF (21). It is difficult to differentiate ECD from mediastinitis (chronic granulomatous, fibrosing, or carcinomatous) or lymphoma when the superior vena cava and/or pulmonary arteries are compressed by the superior vena cava and/or pulmonary arteries (3). It needs to be differentiated in relation to pathology and the involvement of other sites. When the lesions involve the pericardium, ECD may be characterized by pericardial thickening and chronic progressive pericardial effusion with possible cardiac tamponade. Pseudotumor of the lateral wall of the right atrium and the right atrioventricular groove may occur in myocardial involvement, the latter of which may encircle the right coronary artery and lead to myocardial infarction (rare but with high mortality). Other cardiac manifestations include arrhythmias and heart failure (14,22,23). Since the clinical manifestations of cardiac involvement are usually not evident, as in the present patient and the involvement is often associated with a poor prognosis, systematic cardiac evaluation should be performed using MRI and CT (5,8,20). Integrated echo and cardiac MRI can recognize constriction and characterize pericardial tissue with high sensitivity and specificity (14). The presence of 'coated aorta', pericardial thickening, pericardial effusion, right atrioventricular groove pseudotumor, encapsulated right coronary artery, and left ventricular diastolic insufficiency on imaging in the present case are all consistent with cardiovascular involvement in ECD. Pleural effusion was also present, possibly related to ECD lung involvement (5).

Of patients with ECD, >30% may present with pseudo 'RPF,' which presents as a perirenal mass. This may lead to proximal ureteral obstruction and hydronephrosis, resulting in dysuria and urinary urgency (24). Retroperitoneal involvement in ECD needs to be differentiated from idiopathic retroperitoneal fibrosis (IRF) and IgG4-related RPF because of the perinephric soft tissue rind manifestations. The main components of IRF are fibrotic and inflammatory infiltrating cells, which usually involve the anterolateral aspect of the abdominal aorta and iliac arteries, wrapping around the distal ureter and leading to manifestations, such as ureteral obstruction and oliguria, but rarely affect the perirenal space. Lesion tissues of IRF can also involve the inferior vena cava, usually causing stenosis and occlusion (22,25). Treatment

consists mainly of surgical interventions to relieve ureteral obstruction and pharmacologic therapy to induce remission of fibroinflammation. Early application of glucocorticoids rapidly relieves inflammation and promotes shrinkage of the mass (26). The long-term use of glucocorticoids is limited by adverse effects; therefore, immunosuppressive agents, such as cyclophosphamide, azathioprine, methotrexate, cyclosporine and tamoxifen can be selected as combinations for recurrent or maintenance therapy for IRF (25,27). However, there is no consensus regarding the choice of immunosuppressive agents. Wang *et al* (26), found that the application of a combination of hormones and cyclophosphamide and the addition of tamoxifen according to the patient's condition, resulted in a reduction of the mass in most patients (27). At the time of diagnosis of RPF in the present patient, tamoxifen, which has anti-inflammatory and antifibrotic effects and is well tolerated, was chosen as a co-administration and cyclophosphamide added when CT suggested that the mass was not shrinking. IgG4-related disease is a fibroinflammatory disease with typical pathologic features of massive IgG4-positive plasma cell infiltration and storiform fibrosis in the diseased tissue, as well as serologic IgG4 positivity in some patients. Among them, IgG4-related RPF commonly involves the abdominal aorta and anterior lateral iliac artery and rarely involves the perinephric and proximal ureters as in ECD (28,29). Additionally, IgG4-related diseases do not usually involve bones (4). Contrastingly, the perinephric infiltration in the present patient is a highly prevalent (68% of cases) as is the characteristic radiographic manifestation of ECD, which appears as a 'hairy kidney' on CT (8,24). Its lesion tissues may directly infiltrate the renal pelvis and proximal ureter, leading to manifestations, such as dysuria and oliguria, while the distal ureter and pelvic cavity are usually unaffected and rarely involve the inferior vena cava (4,22). When RPF with atypical clinical presentation and imaging is encountered, the possibility of ECD needs to be considered, and further pathological examination is recommended to exclude other diseases. Palliative percutaneous nephrostomies can be selected for patients with renal involvement to preserve renal function (30).

Additionally, retro-orbital infiltration may manifest as bilateral exophthalmos, and endocrine involvement most frequently manifests as diabetes insipidus. Neurological involvement may manifest as cerebellar and pyramidal syndromes and skin involvement may present as macular

Table I. Clinical features of ECD, LCH and RDD (2,4,8,10,23).

Clinical feature	ECD	LCH	RDD
Bone	95%. Bilateral, symmetric cortical osteosclerosis of the diaphyseal and metaphyseal regions. Only 50% of patients describe bone pain	80%. Osteolytic lesions of calvarium, facial bones, proximal limbs, pelvis and scapula. Lytic skull lesions in children are the most common, which may be asymptomatic	5-10%. Osteolytic or sclerotic or mixed lysogenic changes of the long bones, vertebrae, or sacrum, often accompanied by LN changes. Bone pain is common
Retroperitoneum	1/3. Perinephric infiltration leading to hydronephrosis and ureteral narrowing. 'Hairy kidney' on CT	Reported, but featureless	4%. Reported, but featureless
Cardiovascular	40-70%. Pericarditis, pericardial effusion, cardiac tamponade, pseudotumor of the right atrium or right atrioventricular groove. 'Coated aorta' on CT	Reported, but featureless	0.1-0.2%. Rare and uncharacteristic
Skin	Xanthelasma (usually involving the eyelids or periorbital spaces)	33%. Scaly erythematous patches, Birbeck granules on electron microscopy	10%. slow-progressing, painless, nonpruritic reddish-brown nodules, plaques, or papules, which may appear throughout the body
LN	Reported, but featureless	5-10%. Uncommon but constitutes high-risk disease	57%. Bilateral painless cervical LN enlargement or palpable masses in other LN sites
CNS	25-50%. Tumor or degenerative lesions; acute headache, elevated intracranial pressure, cone system response, cognitive or behavioral disorders	Pituitary lesions (25%). Others (2-4%); cerebellar or brain stem lesions, dural-based lesions, brain parenchymal lesions, and non-infiltrative neurodegeneration	<5%. Dural-based mass
Orbit	Retro orbital xanthelasma, exophthalmos	Rare	11%. Orbital mass
Lungs	50%. Asymptomatic and normal on plain films. HRCT shows thickening of interlobular septal, ground-glass opacities, or centrilobular opacities, pleural thickening, or pleural effusion	15%. Nodular and cystic changes in upper and middle lobes on CT	2%. Pulmonary nodular consolidation in lobes of the lungs on CT. Involvement of lower respiratory tract has 45% mortality rate
Liver and spleen	Rare	15%. Uncommon but constitutes high-risk disease	Reported, but featureless
Endocrine	25%. DI	20%. DI, growth hormone deficiency, or panhypopituitarism with hypo thalamic syndrome	Rare

ECD, Erdheim-Chester disease; LCH, Langerhans cell histiocytosis; RDD, Rosai-Dorfman disease; LN, lymph nodes; CNS, central nervous system; CT, computed tomography; HRCT, high resolution CT; DI, diabetes insipidus.

tumors in the orbital or periorbital space. Since these manifestations were not found in the present patients, they will not be discussed in detail.

As shown in Table I, 20% of ECD characteristics can overlap with those of LCH; however, the two diseases are very different in terms of pathology, clinical features and radiologic

manifestations (9). The Langerhans histiocytes of LCH tend to migrate or differentiate from bone marrow-derived monocyte or dendritic cells. Contrastingly, the histiocytes of ECD are mostly associated with bone marrow-derived monocytes. Histiocyte staining for CD1a-positive and CD207-positive can provide evidence of LCH (2,4,9). LCH most commonly

occurs in children and can involve bones throughout the body in 80% of cases, with radiographic manifestations of osteolytic changes (2,8,9). Furthermore, skin involvement manifests as red papules in the groin, chest, abdomen and back, which can be differentiated from cutaneous xanthomas in ECD (8). RDD is also a non-Langerhans histiocytosis, which is more common in children and young adults (2,6,31). The pathological hallmark is the accumulation of characteristic S100-positive large histiocytes showing frequent emperipolesis (i.e., the cells are phagocytosed by the RDD histiocyte and still survive and can exit the histiocytes) and IHC showing positivity for CD68, CD163 and S100, and negativity for CD1a and CD207 (2,8,9,31). The main clinical manifestations are bilateral painless cervical lymphadenopathy (57%) and palpable masses in other lymphatic sites (9,31). Extra-lymph node involvement, including osteolytic or sclerotic changes in the bone, slow-progressing and painless skin nodules or rashes and pulmonary nodular solid lesions, can occur in 43% of cases. However, such symptoms lack typical radiologic features. Cardiovascular and retroperitoneal area involvement is very rare in both LCH and RDD (8,9,31). Considering this, the present case did not fit the typical presentation of LCH and RDD, and these conditions were excluded as possible diagnoses.

Imaging examination is crucial for the diagnosis of ECD. As retroperitoneal and vascular involvement are often asymptomatic, all patients with clinical suspicion of ECD should undergo thoracoabdominal CT (21). If the economic status of the patient permits, 18F-fluorodeoxyglucose positron emission tomography/CT (18F-FDG PET/CT) should be performed 3-6 months after the initiation of therapy to evaluate the metabolic response of ECD (3,32,33). Identifying bone and bone marrow involvement and confirming the area for CT-guided percutaneous biopsy may be important in cases of extraskeletal involvement (32). For patients who have already undergone FDG PET/CT before biopsy, Goyal *et al* (3) recommend a biopsy of most FDG-avid sites that are accessible and safe, especially in cases of bony lesions.

The 5-year survival rate for ECD is 68%, and the primary causes of death include respiratory distress, pulmonary fibrosis and heart failure (5). The choice of therapy should be individualized according to the characteristics of the involved organs, disease progression and type of gene mutation. Currently, IFN- α and PEG-IFN- α are the first-line drugs for the treatment of ECD (3). There are no significant differences in the potential side effects of these two drugs, which include fever, flu-like symptoms, muscle pain and arthralgia, neurological symptoms, gastrointestinal symptoms and myelosuppression. Notably, IFN- α has emerged as an independent prognostic indicator of improved survival in a multivariate analysis (34). It may exert beneficial effects within patients with ECD by inducing the maturation and activation of dendritic cells, immune-mediated histiocyte destruction, or direct resistance to tissue cell proliferation (9,35). Nevertheless, PEG-IFN- α is generally considered to have improved toleration (9) while being easily applicable for once-weekly administration. Therefore, it is recommended that the patient receive PEG-IFN- α treatment. Due to the short duration of the treatment, further follow-up is required to fully investigate the efficacy and prognosis.

The present study presented a case of ECD involving multiple organs. Due to the inadequate knowledge of ECD,

it failed to find the few foam cells on the second pathology result of the patient in time, which delayed the diagnosis. The following possibilities were considered as reasons for the low number of typical pathologic cells of this patient: i) The patient may have had a type of ECD that lacks typical histiocytes; ii) due to the delayed diagnosis, the lesion tissues have developed into dense fibrosis and the puncture needle was unable to reach deeper tissues; therefore, the tissue obtained was atypical; iii) the pathological tissues obtained were too small to detect sufficient lesion cells; iv) long-term hormone and immunosuppressant therapy may have masked the real condition of the patient. The present case showed that clinicians must increase their knowledge of ECD to improve diagnostic sensitivity and accuracy. In clinical practice, the possibility of ECD should be considered if manifestations, such as osteosclerosis (especially symmetrical long bone changes), 'hairy kidney,' 'coated aorta' and pericardial effusion of unknown etiology, are encountered. Such patients should be subjected to systemic screening as early as possible, aggressive biopsy of tissues from all lesions, and refinement of genetic tests to clarify the diagnosis and guide clinical treatment at an early stage. Even if the pathological presentation is not sufficiently typical, ECD cannot be completely excluded, and a comprehensive judgment should be made in conjunction with clinical and imaging studies, and other diseases should be ruled out. This study has several limitations. First, due to the rarity of ECD, most available data are obtained from case reports, and our knowledge of ECD is lacking. Second, although a final diagnosis was made, the lack of genetic evidence limited the treatment options. In the future, longer follow-ups of the patient will be performed to observe the local and systemic status and provide timely therapeutic interventions.

Acknowledgements

Not applicable.

Funding

The present study was supported by the Special Fund for Flow Cytometry Lymphocyte Subgroups of Shandong Provincial Medical Association (grant no. YXH2022ZX03223), the Open Project of Shandong Key Laboratory of Rheumatic Disease and Translational medicine (grant no. QYKFKT2023-7) and China Zhongguancun Precision Medicine Science and Technology Foundation (grant no. RCTAIIRSLE021).

Availability of data and materials

The data generated in the present study may be requested from the corresponding author.

Authors' contributions

XS designed the study, drafted and revised the manuscript, created and revised illustrations. GS provided substantial contributions to critically revising the manuscript for important intellectual content. MX contributed substantially by obtaining the patients' medical records and revising the manuscript. TL and YL contributed substantially to obtaining

and revising medical images. YH and ZW collected clinical data of the patient, and confirm the authenticity of all the raw data. All authors read and approved the final version of the manuscript.

Ethics approval and consent to participate

Not applicable.

Patient consent for publication

Not applicable.

Competing interests

The authors declare that they have no competing interests.

References

1. Khoury JD, Solary E, Ablu O, Akkari Y, Alaggio R, Apperley JF, Bejar R, Berti E, Busque L, Chan JKC, *et al*: The 5th edition of the World Health Organization Classification of Haematolymphoid Tumours: Myeloid and histiocytic/dendritic neoplasms. *Leukemia* 36: 1703-1719, 2022.
2. Emile JF, Cohen-Aubart F, Collin M, Fraitag S, Idbaih A, Abdel-Wahab O, Rollins BJ, Donadieu J and Haroche J: Histiocytosis. *Lancet* 398: 157-170, 2021.
3. Goyal G, Heaney ML, Collin M, Cohen-Aubart F, Vaglio A, Durham BH, Herschkovitz-Rokah O, Girschikofsky M, Jacobsen ED, Toyama K, *et al*: Erdheim-Chester disease: Consensus recommendations for evaluation, diagnosis, and treatment in the molecular era. *Blood* 135: 1929-1945, 2020.
4. Haroche J, Cohen-Aubart F, Rollins BJ, Donadieu J, Charlotte F, Idbaih A, Vaglio A, Abdel-Wahab O, Emile JF and Amoura Z: Histiocytoses: Emerging neoplasia behind inflammation. *Lancet Oncol* 18: e113-e125, 2017.
5. Campochiaro C, Tomelleri A, Cavalli G, Berti A and Dagna L: Erdheim-Chester disease. *Eur J Intern Med* 26: 223-229, 2015.
6. McClain KL, Bigenwald C, Collin M, Haroche J, Marsh RA, Merad M, Picarsic J, Ribeiro KB and Allen CE: Histiocytic disorders. *Nat Rev Dis Primers* 7: 73, 2021.
7. Cao XX, Sun J, Li J, Zhong DR, Niu N, Duan MH, Liang ZY and Zhou DB: Evaluation of clinicopathologic characteristics and the BRAF V600E mutation in Erdheim-Chester disease among Chinese adults. *Ann Hematol* 95: 745-750, 2016.
8. Diamond EL, Dagna L, Hyman DM, Cavalli G, Janku F, Estrada-Veras J, Ferrarini M, Abdel-Wahab O, Heaney ML, Scheel PJ, *et al*: Consensus guidelines for the diagnosis and clinical management of Erdheim-Chester disease. *Blood* 124: 483-492, 2014.
9. Papo M, Cohen-Aubart F, Trefond L, Bauvois A, Amoura Z, Emile JF and Haroche J: Systemic Histiocytosis (Langerhans cell histiocytosis, Erdheim-Chester disease, Destombes-Rosai-Dorfman disease): From oncogenic mutations to inflammatory disorders. *Curr Oncol Rep* 21: 62, 2019.
10. Cohen Aubart F, Emile JF, Carrat F, Charlotte F, Benamer N, Donadieu J, Maksud P, Idbaih A, Barete S, Hoang-Xuan K, *et al*: Targeted therapies in 54 patients with Erdheim-Chester disease, including follow-up after interruption (the LOVE study). *Blood* 130: 1377-1380, 2017.
11. Campochiaro C, Cavalli G, Farina N, Tomelleri A, De Luca G and Dagna L: Efficacy and improved tolerability of combination therapy with interleukin-1 blockade and MAPK pathway inhibitors for the treatment of Erdheim-Chester disease. *Ann Rheum Dis* 81: e11, 2022.
12. Arnaud L, Hervier B, Néel A, Hamidou MA, Kahn JE, Wechsler B, Pérez-Pastor G, Blomberg B, Fuzibet JG, Dubourguet F, *et al*: CNS involvement and treatment with interferon- α are independent prognostic factors in Erdheim-Chester disease: A multicenter survival analysis of 53 patients. *Blood* 117: 2778-2782, 2011.
13. Miller RC, Villà S, Kamer S, Pasquier D, Poortmans P, Micke O and Call TG: Palliative treatment of Erdheim-Chester disease with radiotherapy: A rare cancer network study. *Radiother Oncol* 80: 323-326, 2006.
14. Palmisano A, Campochiaro C, Vignale D, Tomelleri A, De Luca G, Bruno E, Monti CB, Cavalli G, Dagna L and Esposito A: Cardiovascular involvement in Erdheim-Chester diseases is associated with myocardial fibrosis and atrial dysfunction. *Radiol Med* 128: 456-466, 2023.
15. Bartoli L, Angeli F, Stefanizzi A, Fabrizio M, Paolisso P, Bergamaschi L, Broccoli A, Zinzani PL, Galì N, Rucci P, *et al*: Genetics and clinical phenotype of Erdheim-Chester disease: A case report of constrictive pericarditis and a systematic review of the literature. *Front Cardiovasc Med* 9: 876294, 2022.
16. De Abreu MR, Chung CB, Biswal S, Haghighi P, Hesselink J and Resnick D: Erdheim-Chester disease: MR imaging, anatomic, and histopathologic correlation of orbital involvement. *AJNR Am J Neuroradiol* 25: 627-630, 2004.
17. Hervier B, Haroche J, Arnaud L, Charlotte F, Donadieu J, Néel A, Lifermann F, Villabona C, Graffin B, Hermine O, *et al*: Association of both Langerhans cell histiocytosis and Erdheim-Chester disease linked to the BRAFV600E mutation. *Blood* 124: 1119-1126, 2014.
18. Wang F, Cao X, Niu N, Zhang Y, Wang Y, Feng F and Jin Z: Multisystemic imaging findings in Chinese patients with Erdheim-Chester disease. *AJR Am J Roentgenol* 213: 1179-1186, 2019.
19. Haroche J, Arnaud L, Cohen-Aubart F, Hervier B, Charlotte F, Emile JF and Amoura Z: Erdheim-Chester disease. *Curr Rheumatol Rep* 16: 412, 2014.
20. Brun AL, Touitou-Gottenberg D, Haroche J, Toledano D, Cluzel P, Beigelman-Aubry C, Piette JC, Amoura Z and Grenier PA: Erdheim-Chester disease: CT findings of thoracic involvement. *Eur Radiol* 20: 2579-2587, 2010.
21. Nikpanah M, Kim L, Mirmomen SM, Symons R, Papageorgiou I, Gahl WA, O'Brien K, Estrada-Veras JI and Malayeri AA: Abdominal involvement in Erdheim-Chester disease (ECD): MRI and CT imaging findings and their association with BRAF^{V600E} mutation. *Eur Radiol* 28: 3751-3759, 2018.
22. Dion E, Graef C, Haroche J, Renard-Penna R, Cluzel P, Wechsler B, Piette JC and Grenier PA: Imaging of thoracoabdominal involvement in Erdheim-Chester disease. *AJR Am J Roentgenol* 183: 1253-1260, 2004.
23. Gianfreda D, Palumbo AA, Rossi E, Buttarelli L, Manari G, Martini C, De Filippo M and Vaglio A: Cardiac involvement in Erdheim-Chester disease: An MRI study. *Blood* 128: 2468-2471, 2016.
24. Chazal T, Pegoraro F, Manari G, Bettiol A, Maniscalco V, Gelain E, Charlotte F, Mazar RD, Renard-Penna R, Amoura Z, *et al*: Clinical phenotypes and long-term outcome of kidney involvement in Erdheim-Chester histiocytosis. *Kidney Int* 103: 177-186, 2023.
25. Vaglio A, Palmisano A, Alberici F, Maggiore U, Ferretti S, Cobelli R, Ferrozzi F, Corradi D, Salvarani C and Buzio C: Prednisone versus tamoxifen in patients with idiopathic retroperitoneal fibrosis: An open-label randomised controlled trial. *Lancet* 378: 338-346, 2011.
26. Wang DL, Liu SB, Feng YC, Li J, Zhang T, Wan L and Gao H: Corticosteroid combined with cyclophosphamide in the patients with retroperitoneal fibrosis: A clinical features and prognostic analysis. *J Clin Med* 17: 18-22, 2019.
27. van Bommel EF, Pelkmans LG, van Damme H and Hendriks TR: Long-term safety and efficacy of a tamoxifen-based treatment strategy for idiopathic retroperitoneal fibrosis. *Eur J Intern Med* 24: 444-450, 2013.
28. Marando A, D'Ambrosio G, Catanzaro F, La Rosa S and Sessa F: IgG4-related disease of the ureter: Report of two cases and review of the literature. *Virchows Arch* 462: 673-678, 2013.
29. Deshpande V, Zen Y, Chan JK, Yi EE, Sato Y, Yoshino T, Klöppel G, Heathcote JG, Khosroshahi A, Ferry JA, *et al*: Consensus statement on the pathology of IgG4-related disease. *Mod Pathol* 25: 1181-1192, 2012.
30. Verdalles U, Goicoechea M, García de Vinuesa S, Mosse A and Luño J: Erdheim-Chester disease: A rare cause of renal failure. *Nephrol Dial Transplant* 22: 1776-1777, 2007.
31. Elbaz Younes I, Sokol L and Zhang L: Rosai-Dorfman disease between proliferation and neoplasia. *Cancers (Basel)* 14: 5271, 2022.
32. Balink H, Hemmelder MH, de Graaf W and Grond J: Scintigraphic diagnosis of Erdheim-Chester disease. *J Clin Oncol* 29: e470-e472, 2011.
33. Lin E: FDG PET/CT for biopsy guidance in Erdheim-Chester disease. *Clin Nucl Med* 32: 860-861, 2007.

34. Hervier B, Arnaud L, Charlotte F, Wechsler B, Piette JC, Amoura Z and Haroche J: Treatment of Erdheim-Chester disease with long-term high-dose interferon- α . *Semin Arthritis Rheum* 41: 907-913, 2012.
35. Braiteh F, Boxrud C, Esmali B and Kurzrock R: Successful treatment of Erdheim-Chester disease, a non-Langerhans-cell histiocytosis, with interferon-alpha. *Blood* 106: 2992-2994, 2005.



Copyright © 2024 Shi et al. This work is licensed under a Creative Commons Attribution-NonCommercial-NoDerivatives 4.0 International (CC BY-NC-ND 4.0) License.